



ELSEVIER

## Matching a transducer to water at cavitation: Acoustic horn design principles

Sergei L. Peshkovsky, Alexey S. Peshkovsky \*

*Industrial Sonomechanics, LLC, 1505 St. Nicholas Avenue #5B, New York, NY 10033, USA*

Received 14 February 2006; received in revised form 6 June 2006; accepted 1 July 2006

### Abstract

High-power ultrasound for several decades has been an integral part of many industrial processes conducted in aqueous solutions. Maximizing the transfer efficiency of the acoustic energy between electromechanical transducers and water at cavitation is crucial when designing industrial ultrasonic reactors with large active volumes. This can be achieved by matching the acoustic impedances of transducers to water at cavitation using appropriately designed ultrasonic horns. In the present work, a set of criteria characterizing the matching capabilities of ultrasonic horns is developed. It is shown that none of the commonly used tapered-shape horns can achieve the necessary conditions. An analytical method for designing five-element acoustic horns with the desirable matching properties is introduced, and five novel types of such horns, most suitable for practical applications, are proposed. An evaluation of the horns' performance is presented in a set of experiments, demonstrating the validity of the developed theoretical methodology. Power transfer efficiency increase by almost an order of magnitude is shown to be possible with the presented horn designs, as compared to those traditionally utilized.

© 2006 Elsevier B.V. All rights reserved.

**Keywords:** Ultrasonic rod horns; Electromechanical transducers; Acoustic impedance matching; Ultrasonic power transference; Acoustic energy transference; Acoustic horns; Industrial ultrasonic reactors; Sonochemistry; Industrial processes in liquids; Cavitation

### 1. Introduction

High-power ultrasound for several decades has been an integral part of many industrial processes conducted in weak aqueous solutions, such as cleaning, extraction, homogenizing, emulsification, sonochemistry, pollutant destruction, etc. [1–3]. These ultrasound-aided (macrosonics) processes are based on the effect of acoustic cavitation induced in water during intensive ultrasonic treatment. The electromechanical transducers used to convert the high frequency electric power into the ultrasonic power cannot, however, directly provide the necessary amplitudes of longitudinal ultrasonic vibrations to induce cavitation. Acoustic rod horns connected to the transducers are, therefore, used to amplify the vibration amplitude. Commonly used acous-

tic horns have tapered shapes, such as conical, exponential, catenoidal, stepped, or more complex, and converge in the direction of the loads [3–5]. Although widely used, these horns suffer from an important limitation: they are incapable of providing matching between the transducers and the aqueous loads, leading to an inefficient acoustic power transmission.

It is well known that for an optimal operation of an ultrasonic horn system, the maximum cross-sectional dimension of any portion of the resonant horn or transducer cannot exceed, approximately, a quarter-wavelength of the corresponding longitudinal acoustic wave at the horn's resonance frequency [6]. Consequently, a convergent horn with a maximal allowed base-width always ends up having a working tip dimension that is smaller than this limitation. The final size of the tip depends on the gain factor of the horn, and becomes reduced as the gain factor increases. This is problematic when the abovementioned processes are carried

\* Corresponding author.

E-mail address: [alexey@sonomechanics.com](mailto:alexey@sonomechanics.com) (A.S. Peshkovsky).

55 out on an industrial scale, since a deposition of substantial  
 56 acoustic power is needed to create acoustic cavitation in  
 57 large volumes of water. While using the converging horns  
 58 permits increasing the specific acoustic power (or vibration  
 59 amplitude) radiated by the electromechanical transducer  
 60 into the load quite effectively, it is impossible to achieve  
 61 the technologically necessary levels of total radiated acous-  
 62 tic power, since the cross-sectional area of the horn tip in  
 63 contact with the load is small. Therefore, it is intuitive that  
 64 the use of the convergent horns does not permit transferring  
 65 all available power of an acoustic transducer into a load.

66 In actual practice a technique that is frequently  
 67 attempted to circumvent this limitation is the use of a con-  
 68 vergent horn with an extension in the form of a small disk at  
 69 the end. This horn, however, usually works inadequately  
 70 because when a disk of arbitrary dimensions is connected  
 71 to a horn, the resonance frequency and the vibration ampli-  
 72 tude conditions change dramatically, in comparison with  
 73 the calculated values, and the horn's behavior becomes dif-  
 74 ficult to predict. Complicated experimental fitting of the  
 75 parameters is then required for each horn. Additionally,  
 76 the fatigue strength of the disk joint is low, which dimin-  
 77 ishes the horn's reliability and lifetime of operation. Rod  
 78 horns connected to planar resonant systems, such as large  
 79 discs or planes are also sometimes used [7]. Another solu-  
 80 tion attempted in the past was to develop an alternative  
 81 reactor design with an incorporated converging horn [3].

82 In this manuscript we introduce novel design principles  
 83 used for the development of a completely novel family of  
 84 acoustic horns, whose shapes permit achieving high gain  
 85 factors and large output surfaces simultaneously. These  
 86 horns can be designed to accurately match an ultrasonic  
 87 source to a liquid (water) load at cavitation, maximizing  
 88 the transference of the available acoustic energy into the  
 89 load and creating a large cavitation volume. The devices  
 90 are easy to machine and have well-isolated axial resonances  
 91 and uniform output amplitudes, as shown in the experimen-  
 92 tal section.

93 **2. Criteria for matching a magnetostrictive transducer to**  
 94 **water at cavitation**

95 Under the most convenient approximation, which is,  
 96 nevertheless, quite suitable for the engineering calculations,  
 97 the highest specific acoustic power that a well (perfectly)  
 98 cooled resonant magnetostrictive transducer can transmit  
 99 into a load is limited by two main factors – the magneto-  
 100 strictive stress saturation,  $\tau_m$  (the maximal mechanical  
 101 stress achievable due to the magnetostrictive effect for a  
 102 given transducer material), and the maximum allowed  
 103 oscillatory velocity, limited by the fatigue strength of the  
 104 transducer material,  $V_m$ , such that [8]

$$\tau_m = e_m E \phi_1 \tag{1}$$

$$V_m = \sigma_m \phi_2 / \rho c$$

107 where  $e_m$  is the deformation amplitude associated with  $\tau_m$ ,  
 108  $E$  is Young's modulus,  $\phi_1$  and  $\phi_2$  are the coefficients that

take into account the features of the transducer construc- 109  
 tion [4,8],  $\sigma_m$  is the stress amplitude of the material fatigue 110  
 strength,  $\rho$  is the transducer material's density, and  $c$  is the 111  
 thin-wire speed of sound in the material. The highest spec- 112  
 ific power radiated under conditions of perfect matching 113  
 between the transducer and the load is represented by the 114  
 quantity 115

$$W_m = 0.5 \tau_m V_m \tag{2}$$

116 Let us now consider the criteria, upon which an ultra- 117  
 sonic horn should be designed in order to achieve a match- 118  
 ing condition between a transducer and a given load. As an 119  
 acoustic load of the transducer, water at cavitation will be 120  
 further considered as the most common and experimentally 121  
 studied load encountered in technological applications of 122  
 ultrasound. It should be noted that the acoustic load under 123  
 consideration, water at cavitation, has a purely active char- 124  
 acter [9], and, therefore, is appropriately described by the 125  
 term "acoustic resistivity",  $r_w$ . Practically, this means that 126  
 virtually all of the acoustic energy deposited into water at 127  
 cavitation is converted into heat [10]. Under the term 128  
 "matching" we will further mean supplying an electromechan- 129  
 ical transducer with a multi-element ultrasonic horn 130  
 possessing a gain factor,  $G \gg 1$  ( $G$  is defined as a ratio of 131  
 the output to input oscillatory velocities,  $V/V_m$ ), which 132  
 allows the transference of a maximum of the available 133  
 acoustic power of the transducer,  $W_m$ , into the load. 134  
 135

Specific acoustic power,  $W_1$ , generated in a purely active 136  
 load by the longitudinal vibrations of an acoustic rod horn 137  
 with an output oscillatory velocity,  $V$ , is represented by 138  
 139

$$W_1 = 0.5 r_w V^2 \tag{3}$$

Taking  $W_m = W_1$  as a matching condition, we obtain 142  
 143

$$\frac{\tau_m}{r_w V} = GN^2 \tag{4}$$

144 where  $N^2 = S_{out}/S_{in}$ ,  $S_{in}$  and  $S_{out}$  are, respectively, the in- 145  
 put and the output cross-sections of the acoustic horn, 146  
 while  $S_m$  is taken to be equal to the output cross-section 147  
 of the electromechanical transducer,  $S_t$  (please see Fig. 1), 148  
 The left-hand side of Eq. (4) reflects the degree of under- 149  
 loading of an acoustic transducer, and the right-hand side 150  
 describes matching capabilities of an acoustic horn. 151  
 152

For a resonant system matched to an acoustic load, the 153  
 traveling-wave factor can be presented as the ratio of the 154  
 maximum energy radiated into the load to the maximum 155

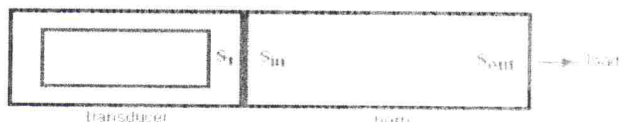


Fig. 1. General schematic is shown, describing matching between an electromechanical transducer and a load achieved by using an acoustic rod horn of an arbitrary shape.  $S_{in}$  and  $S_{out}$  are, respectively, the input and the output cross-sections of the acoustic horn;  $S_t$  is the output cross-section of the electromechanical transducer.



156 energy stored in the transducer in the form of a standing  
157 acoustic wave

$$159 \quad k_1 = \frac{\tau_m V_m}{\rho c V_m^2} = \frac{\tau_m}{\sigma_m \phi_2} \quad (5)$$

160 For the common magnetostrictive materials,  $\tau_m$  is much  
161 smaller than  $\sigma_m$ , and, therefore,  $k_1 \ll 1$ . This means  
162 that a standing-wave mode in the transducer matched  
163 to the load is always present. In addition, since the  
164 considered acoustic load has an active character, the reso-  
165 nance dimensions of the transducer and the horn are  
166 preserved.

167 From experimental studies [9] it is known that during  
168 the radiation of ultrasound into water at cavitation, the  
169 relationship  $r_w V = \sqrt{2} P_0$ , where  $P_0$  is the hydrostatic pres-  
170 sure of water, remains, roughly, constant. Therefore, the  
171 following can be written:

$$172 \quad \frac{\tau_m}{r_w V} = \frac{c_m E \phi_1}{\sqrt{2} P_0} \quad (6)$$

175 It is seen from Eq. (6) that the degree of the under-loading  
176 of an acoustic transducer depends only on the characteris-  
177 tics of the transducer itself and the hydrostatic pressure of  
178 water. For most common magnetostrictive materials, the  
179 calculated values of  $\tau_m/r_w V$  are between 15 and 44. In this  
180 calculation, the values of  $P_0 = 10^5 \text{ N/m}^2$  and  $\phi_1 = 0.45$   
181 were assumed.

182 Industrial acoustic transducers, generally, have their  
183 nominal electrical power  $W_e$ , efficiency factor  $\eta$  and output  
184 oscillatory velocity  $V_n$  specified. The practical degree of the  
185 under-loading for such industrial magnetostrictive trans-  
186 ducers can be, therefore, characterized by the relationship  
187  $2\eta W_e/r_w V V_n S_t$ , having assumed that  $W_m = \eta W_e/S_t$ . The  
188 practical values of the degree of under-loading obtained  
189 from this expression are much lower than the correspond-  
190 ing theoretical limits for the magnetostrictive materials  
191 themselves, and for most models fall in the range between  
192 3 and 5.

193 It is important to point out that in the case of piezoelec-  
194 tric transducers the highest achievable level of specific  
195 acoustic power is practically restricted by the electrical  
196 resilience of the entire apparatus, rather than by the prop-  
197 erties of the piezoelectric material itself. The limiting value  
198 of maximal electric power is, generally, available from the  
199 transducer supplier and can also be used in this expression  
200 for the evaluation of the practical degree of under-loading  
201 of the industrial piezoelectric transducers.

202 It is less evident how to use the right-hand side of Eq.  
203 (4), which reflects the matching capabilities of a horn.  
204 The point to emphasize is that in spite of a variety of types  
205 and shapes of the acoustic horns known from the literature  
206 and used in practice, none exist, for which the relationship  
207  $GN^2 > 1$ , when  $G > 1$ , would hold true. It is, therefore,  
208 clear that in order to be able to match ultrasonic transduc-  
209 ers to water at cavitation, it is necessary to develop new

types of acoustic horns that would meet the matching cri- 210  
terion,  $GN^2 > 1$ . 211

### 3. Five-element matching horns 212

#### 3.1. Design principles 213

214 The theory of acoustic horns is based on the problem of  
215 longitudinal vibrations of multi-element rods that have  
216 cylindrical elements and elements of variable cross-sections  
217 [11]. We will consider only the horns of axially symmetric  
218 shapes. Other types of horns (for example, wedge-shaped)  
219 can be considered in the analogous way. In the current  
220 work we will restrict the discussion to the five-element  
221 horns, although no theoretical restriction for the number  
222 of elements exists.

223 We assume that during the passage of the stress waves  
224 through a horn, the wave front remains planar, while the  
225 stresses are uniformly distributed over the horn's cross-  
226 section. This assumption limits us to the thin horns, whose  
227 resonance lengths significantly exceed their diameters. For  
228 all practical purposes, it is sufficient to require that the  
229 maximum cross-sectional dimension of any portion of a  
230 resonant horn not exceed, approximately, a quarter-wave-  
231 length of the corresponding thin wire acoustic wave at the  
232 horn's resonance frequency [6].

233 The schematic and the designation of parameters for a  
234 general case of a five-element rod horn are given in Fig. 2,  
235 where two possible situations are presented: a horn with  
236  $d_1/d_3 > 1$  is shown by the solid line; a horn with  $d_1/d_3 < 1$   
237 is shown by the dotted line. Under the assumed approxima-  
238 tion, the problem is reduced to one-dimension, and it is limited  
239 to the consideration of elements with variable cross-  
240 section of only conical shape. For a steady-state mode,  
241 the equation of vibrations for displacements,  $u$ , takes the  
242 following form: 243

$$244 \quad u'' + \frac{1}{S} S' u' + k^2 u = 0 \quad (7) \quad 245$$

246 where  $k = \omega/c$  is the wave number,  $\omega = 2\pi f$  is the angu-  
247 lar frequency of vibrations, and  $f$  is the frequency of  
248 vibrations.

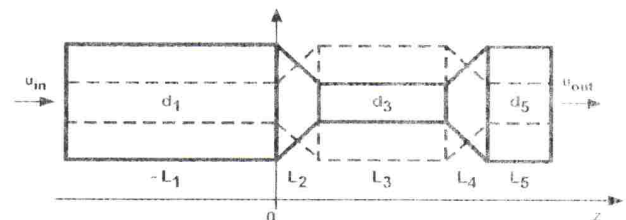


Fig. 2. Schematic defining the parameters of a five-element matching horn is shown. The horn having  $d_1/d_3 > 1$  is shown by a solid line, and the horn with  $d_1/d_3 < 1$  is shown by a dotted line. Parameters  $L_1$ – $L_5$  correspond to the lengths of each element.

249 The solutions of Eq. (7) for each of the horn's elements  
250 can be written as

$$\begin{aligned}
 251 \quad u_1 &= A_1 \cos kz + B_1 \sin kz; \quad -L_1 < z < 0 \\
 u_2 &= F(A_2 \cos kz + B_2 \sin kz); \quad 0 < z < L_2 \\
 u_3 &= A_3 \cos kz + B_3 \sin kz; \quad L_2 < z < L_2 + L_3 \\
 u_4 &= F(A_4 \cos kz + B_4 \sin kz); \quad L_2 + L_3 < z < L_2 + L_3 + L_4 \\
 253 \quad u_5 &= A_5 \cos kz + B_5 \sin kz; \quad L_2 + L_3 + L_4 < z < L_2 + L_3 + L_4 + L_5
 \end{aligned} \tag{8}$$

254 Then, using the boundary conditions for the horn's ele-  
255 ment, we obtain the system of equations for displacements,  
256  $u$ , and strains,  $u'$ .

257 At  $z = -L_1$ ,  $u_1 = u_{in}$ ,  $ES_1 u'_1 = -F_{in}$ ,  $F_{in} = 0$

$$A_1 \cos kL_1 - B_1 \sin kL_1 = u_{in};$$

259  $EkS_1(A_1 \sin kL_1 + B_1 \cos kL_1) = -F_{in}$

260 At  $z = 0$ ,  $u_2 = u_1$ ,  $u'_2 = u'_1$

$$FA_2 = A_1;$$

$$F'A_2 + FB_2 k = kB_1;$$

$$\alpha = (d_1 - d_3)/L_2 d_1;$$

$$F = 2/d_1;$$

262  $F' = F\alpha$

263 At  $z = L_2$ ,  $u_3 = u_2$ ,  $u'_3 = u'_2$

$$\begin{aligned}
 264 \quad A_3 \cos kL_2 + B_3 \sin kL_2 &= F(A_2 \cos kL_2 + B_2 \sin kL_2); \\
 &-kA_3 \sin kL_2 + kB_3 \cos kL_2
 \end{aligned}$$

$$= (F'B_2 - FkA_2) \sin kL_2 + (F'A_2 + FkB_2) \cos kL_2;$$

$$\alpha = (d_1 - d_3)/L_2 d_1;$$

$$F = 2/d_3;$$

266  $F' = -F/(L_2 - 1/\alpha)$  (9)

267 At  $z = L_2 + L_3$ ,  $u_4 = u_3$ ,  $u'_4 = u'_3$

$$\begin{aligned}
 &F[A_4 \cos k(L_2 + L_3) + B_4 \sin k(L_2 + L_3)] \\
 &= A_3 \cos k(L_2 + L_3) + B_3 \sin k(L_2 + L_3); \\
 &(F'B_4 - FkA_4) \sin k(L_2 + L_3) + (F'A_4 + FkB_4) \cos k(L_2 + L_3) \\
 &= -kA_3 \sin k(L_2 + L_3) + kB_3 \cos k(L_2 + L_3);
 \end{aligned}$$

269  $\alpha = (d_3 - d_5)/L_4 d_3$ ;  $F = 2/d_3$ ;  $F' = F\alpha$

270 At  $z = L_2 + L_3 + L_4$ ,  $u_5 = u_4$ ,  $u'_5 = u'_4$

$$\begin{aligned}
 &A_5 \cos k(L_2 + L_3 + L_4) + B_5 \sin k(L_2 + L_3 + L_4) \\
 &= F[A_4 \cos k(L_2 + L_3 + L_4) + B_4 \sin k(L_2 + L_3 + L_4)]; \\
 &-kA_5 \sin k(L_2 + L_3 + L_4) + kB_5 \cos k(L_2 + L_3 + L_4) \\
 &= (F'B_4 - FkA_4) \sin k(L_2 + L_3 + L_4) \\
 &\quad + (F'A_4 + FkB_4) \cos k(L_2 + L_3 + L_4);
 \end{aligned}$$

272  $\alpha = (d_3 - d_5)/L_4 d_3$ ;  $F = 2/d_5$ ;  $F' = -F/(L_4 - 1/\alpha)$

273 At  $z = L_2 + L_3 + L_4 + L_5$ ,  $u_5 = u_{out}$ ,  $u'_5 = 0$

$$\begin{aligned}
 &A_5 \cos k(L_2 + L_3 + L_4 + L_5) + B_5 \sin k(L_2 + L_3 + L_4 + L_5) = u_{out}; \\
 275 \quad &-A_5 \sin k(L_2 + L_3 + L_4 + L_5) + B_5 \cos k(L_2 + L_3 + L_4 + L_5) = 0
 \end{aligned}$$

The gain factor of the horn can be expressed as 276

$$\begin{aligned}
 G &= \left| \frac{u_{out}}{u_{in}} \right| \\
 &= \left| \frac{A_5 \cos k(L_2 + L_3 + L_4 + L_5) + B_5 \sin k(L_2 + L_3 + L_4 + L_5)}{A_1 \cos kL_1 - B_1 \sin kL_1} \right|
 \end{aligned} \tag{10} \quad 278$$

where  $F = 2/d_n$ ,  $d_n$  is the diameter of the corresponding 279  
cylindrical element of the horn,  $A_n$  and  $B_n$  are the constant 280  
coefficients for the corresponding elements of the horn,  $L_n$  281  
is the length of the corresponding element of the horn,  $n$  is 282  
the order number of the horn element,  $z$  is the cone index 283  
of the horn element with variable cross-section,  $u_{in}$  and  $u_{out}$  284  
are the amplitudes of displacements at the horn input and 285  
output, respectively. The boundary conditions for the force 286  
acting on the horn's input,  $F_{in} = 0$ , and for the strain at the 287  
horn output,  $u'_5 = 0$ , in this system of equations indicate 288  
that the horn has a total resonance length and does not 289  
have an acoustic load. 290

From the system of equation (9), one can obtain all necessary 291  
characteristics of a five-element horn: lengths and 292  
diameters of the elements, gain factor, distribution of 293  
vibration amplitudes, and distribution strains along the 294  
horn. From this system of equations, it is also easy to 295  
obtain solutions for any horns with conical elements (for 296  
example, with a number elements smaller than five). Horns 297  
with other shapes of the variable cross-section elements 298  
(for example, with exponential or catenoidal elements) 299  
can be considered in an analogous way, taking into account 300  
the variation of sound velocity in such elements. 301

### 3.2. Analysis of five-element horns 302

To solve the system of Eq. (9) and to present results in a 303  
convenient graphical form, a computer program has been 304  
written that allows all the indicated above characteristics 305  
of five-element horns to be obtained in real time for subse- 306  
quent analysis. The input parameters are: operating fre- 307  
quency of the horn, acoustic properties and fatigue 308  
strength of the horn material, and the diameter-to-length 309  
ratios of the horn elements. 310

Out of all variety of possible types of five-element horns, 311  
let us consider the five horns that are most suitable for practical 312  
applications. For the convenience of a comparison of 313  
horn parameters, we further assume  $N = d_1/d_5 = 1$ . Fig. 3 314  
shows a conical-cylindrical matching horn and its design 315  
parameters. This is the simplest degenerate horn with 316  
 $L_1 = 0$ . Such a horn has low matching capabilities, the maximum 317  
value being  $GN^2 \approx 3$ . 318

Fig. 4 shows a step matching horn and its design parameters. 319  
The maximum value of the matching capability of this horn is 320  
 $GN^2 \approx 4$ . Both horns considered above can 321  
be used to match industrial acoustic transducers of low 322  
power for exciting relatively low amplitudes of ultrasonic 323  
vibrations in the load. Their small resonance dimensions 324  
convenient for construction should be particularly noted. 325

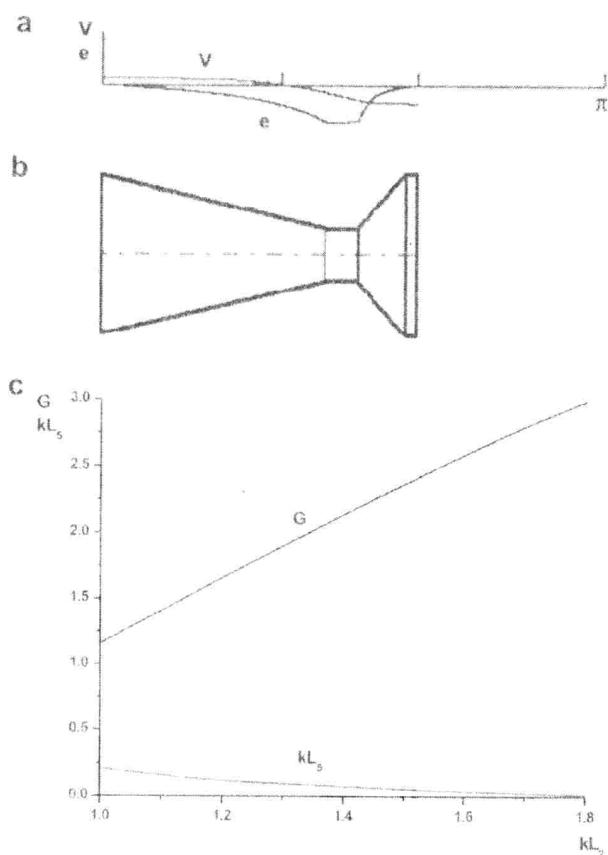


Fig. 3. Conical cylindrical horn is shown with  $d_1 = d_2$ ;  $d_1/d_3 = 3.0$ ;  $kL_1 = 0$ ;  $kL_3 = 0.2$ ;  $kL_4 = 0.3$ , along with (a) the distribution of the oscillatory velocity,  $V$ , and strain,  $e$ , along the horn; (b) drawing of the horn; (c) plot of the distribution of the horn's parameters.

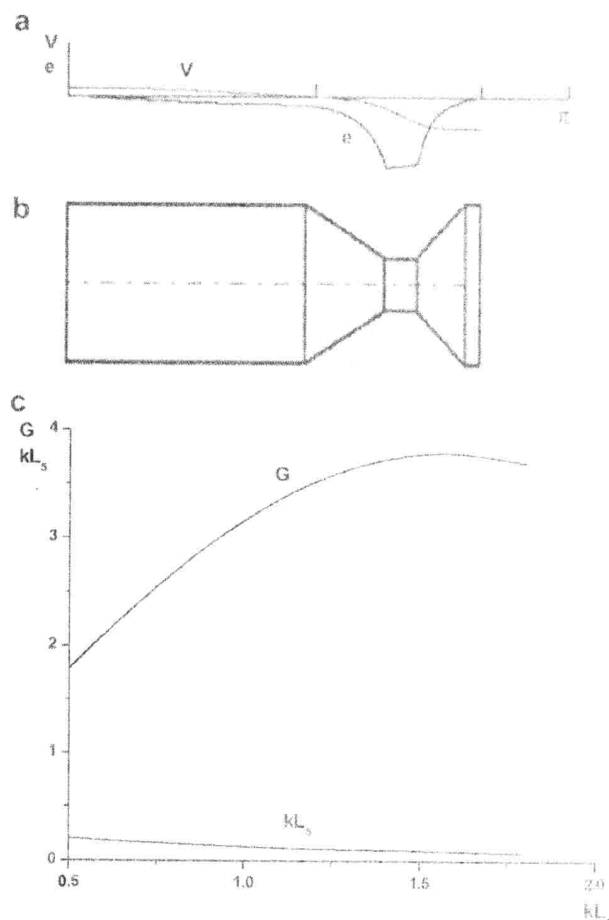


Fig. 4. Stepped horn is shown with  $d_1 = d_2$ ;  $d_1/d_3 = 3.0$ ;  $kL_1 = 0.5$ ;  $kL_3 = 0.2$ ;  $kL_4 = 0.3$ , along with (a) the distribution of the oscillatory velocity,  $V$ , and strain,  $e$ , along the horn; (b) drawing of the horn; (c) plot of the distribution of the horn's parameters.

326 A barrel-shaped matching horn and its design parameters are shown in Fig. 5. This horn is quite promising for the matching of acoustic transducers of small cross dimensions or for the use as a booster. The maximum value of its matching capabilities at the given parameters is  $GN^2 \approx 8$ . It should be borne in mind that the diameter of the horn's heavy section,  $d_3$ , under the considered approximation must not exceed about a quarter of the length of acoustic wave.

335 Fig. 6 shows a spool-shaped matching horn and its design parameters. This horn is atypical because its main radiating surface is lateral, and it mainly radiates a cylindrical wave into the load, as opposed to a plane wave radiated by other matching horns. Given a symmetric form of the horn, the gain factor is always equal to 1, the node of displacements is located in the middle, and lateral surfaces move in anti-phase. When using lateral radiation, the horn's matching capabilities are quite high since there are no limitations on the overall length. Such horn connected into a sequential string can radiate a cylindrical wave of high total power into the load and produce a well-developed cavitation region of a large volume.

348 Above, we have considered the horns whose lengths were less than or close to half the length of the acoustic

350 wave in the rod, the so-called half-wave horns. The system of Eq. (9) also allows one to obtain solutions for full-wave horns. One of such horns intended for the radiation of a plane acoustic wave of a very high power into water is a barbell-shaped horn shown in Fig. 7. Its design parameters, as a function of  $d_1/d_3$ , are presented in Fig. 7(c). The matching capabilities of the barbell-shaped horn can reach the values of  $GN^2 = 20$  or more. Such horn is very promising for the matching of high-power acoustic transducers that have large cross dimensions. For example, the highest design power radiated into the water at cavitation by this horn, made of titanium alloy, taking into account the fatigue strength limitations and limitations on output diameter under normal hydrostatic pressure, is about 5 kW at a frequency of 20 kHz. This value of the power of the acoustic radiation is close to the theoretically attainable maximum under the given conditions for any metallic rod horn. An expression for the theoretically attainable maximum power of acoustic radiation deposited into water under cavitation at a given frequency and electrostatic pressure,  $W = P_0 V_m S_m$ , can be obtained based on expressions 2 and 3,

351  
352  
353  
354  
355  
356  
357  
358  
359  
360  
361  
362  
363  
364  
365  
366  
367  
368  
369  
370

6

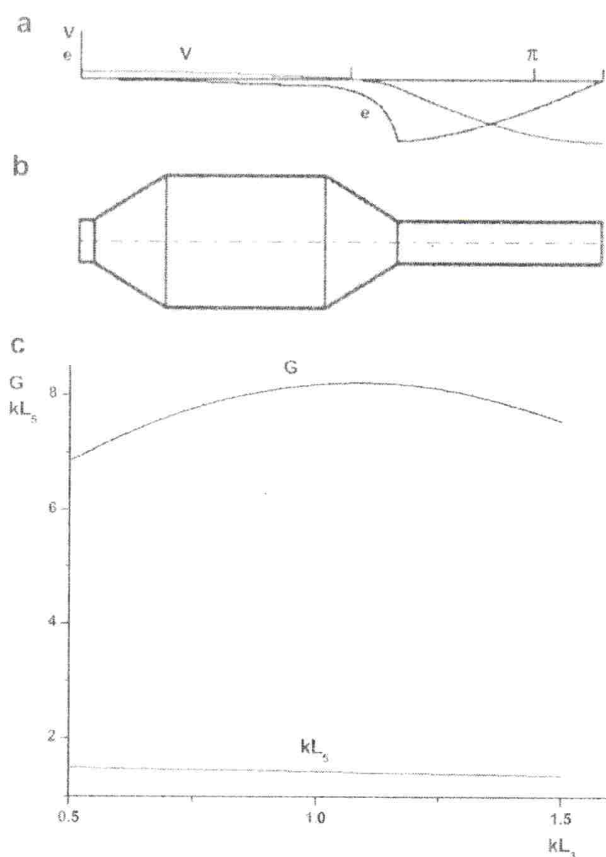


Fig. 5. Barrel horn is shown with  $d_1 = d_5$ ;  $d_3/d_1 = 3.0$ ;  $kL_1 = 0.1$ ;  $kL_2 = kL_4 = 0.5$ , along with (a) the distribution of the oscillatory velocity,  $V$ , and strain,  $e$ , along the horn; (b) drawing of the horn; (c) plot of the distribution of the horn's parameters.

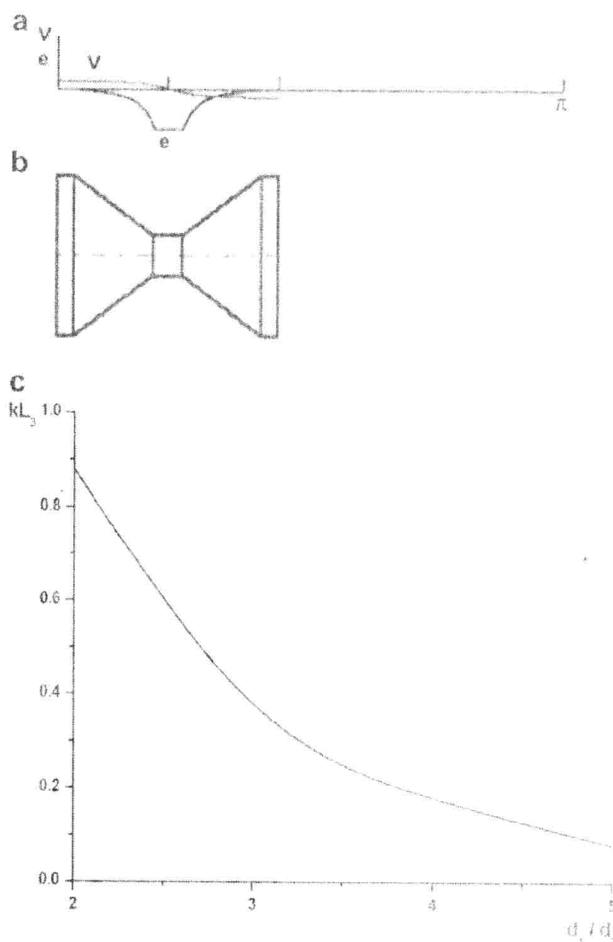


Fig. 6. Symmetrical spool-shaped horn is shown with  $d_1 = d_5$ ;  $kL_1 = kL_5 = 0.1$ ;  $kL_3 = kL_4 = 0.5$ , along with (a) the distribution of the oscillatory velocity,  $V$ , and strain,  $e$ , along the horn; (b) drawing of the horn; (c) plot of the distribution of the horn's parameters.

371 taking into account that  $r_w V = \sqrt{2} P_0$ . Here,  $S_m$  is the  
 372 maximum possible area of the circular output surface of  
 373 the acoustic horn, whose diameter is restricted by the  
 374 quarter-wavelength condition mentioned above. The max-  
 375 imum achievable oscillation velocity,  $V_m$ , for best titanium  
 376 alloys used as horn materials reaches, approximately, 10–  
 377 15 m/s.

378 Due to the significant potential of the barbell-shaped  
 379 horn for the industrial applications of ultrasound, we pro-  
 380 vide its exact parameters in Table 1. These parameters are  
 381 convenient for the use during practical calculations.

382 **3.3. Frequency characteristics of five-element horns**

383 The knowledge of the frequency characteristics of an  
 384 acoustic horn is very important when choosing the type  
 385 of a matching horn for specific conditions of its excitation  
 386 (type of an ultrasonic generator) and operation (properties  
 387 of an acoustic load). These characteristics, according to (8),  
 388 can be obtained by calculation in the form of a frequency  
 389 dependence of the horn's input resistance. If losses are  
 390 ignored, the expression for the input resistance of a five-ele-  
 391 ment horn can be derived from the system of equation (9),  
 392 assuming  $z = F_{in}/j\omega u_{in}$ . Taking  $z_0 = EkS_{in}/\omega$ , one can write

$$\frac{z}{z_0} = \frac{j(A_1 \sin kL_1 + B_1 \cos kL_1)}{A_1 \cos kL_1 - B_1 \sin kL_1} \tag{11}$$

The values of  $|z/z_0|$  for the five-element horns considered  
 395 above were calculated at a small change in the current fre-  
 396 quency  $f$ , as compared with the horn natural frequency  $f_r$ ,  
 397 so that  $(f_r - f)/f_r = 0.02$ . Table 2 gives the values of  $|z/z_0|$   
 398 obtained at the frequency,  $f$ , for the horns shown in Figs.  
 399 3–7 with similar gain factors,  $G \approx 3$  (with the exception  
 400 of the horn in Fig. 6). For comparison, the table also gives  
 401 the values of  $|z/z_0|$  for two resonant cylindrical rods that  
 402 have characteristic lengths  $kL = \pi$  and  $kL = 2\pi$ . It is evi-  
 403 dent that the presented values of  $|z/z_0|$  characterize the rate  
 404 of change in the horn's input resistance with a change in  
 405 the frequency of excitation or the parameters of the acous-  
 406 tic load.  
 407

408 From Table 2 it is seen that the horn shown in Fig. 6 has  
 409 the lowest frequency dependence of the input resistance. It  
 410 is most suitable for the use in a sequentially connected  
 411 string of such horns for the radiation of a cylindrical wave  
 412 into the load. In this case, the low dependence of the horn



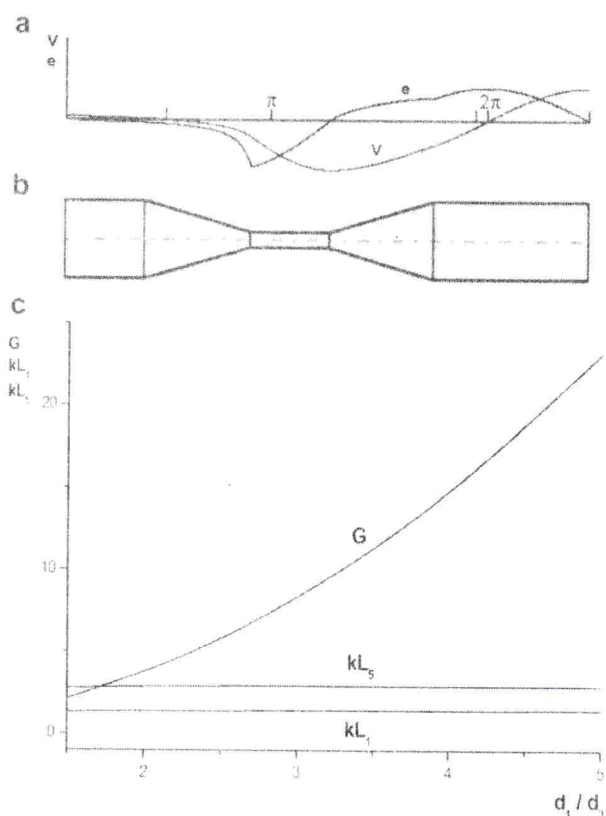


Fig. 7. Barbell-shaped horn is shown with  $d_1 = d_3$ ;  $kL_1 = kL_3$ ;  $kL_2 = kL_4 = 0.5$ , along with (a) the distribution of the oscillatory velocity,  $v$ , and strain,  $e$ , along the horn; (b) drawing of the horn; (c) plot of the distribution of the horn's parameters.

Table 1

$N$	$G$	$kL_1$	$kL_2$	$kL_3$
1.5	2.176	1.383	0.405	2.853
2.0	3.527	1.290	0.693	2.725
2.5	4.918	1.245	0.916	2.640
3.0	6.285	1.224	1.099	2.574
3.5	7.597	1.216	1.253	2.519
4.0	8.834	1.215	1.386	2.470
4.5	9.987	1.217	1.504	2.426
5.0	11.049	1.222	1.609	2.384

Table 2

Horn type	Cylinder $kL = \pi$	Cylinder $kL = 2\pi$	Fig. 3	Fig. 4	Fig. 5	Fig. 6	Fig. 7
$ z/z_0 $	0.063	0.126	0.09	0.14	0.345	0.024	0.67

the horn shown in Fig. 3. The barbell-shaped full-wave horn is characterized by an abrupt dependence of input resistance on frequency. In this case, the positive feature is that a small error in dimensions during manufacturing of the horn has little influence on its resonance frequency. The horn can also reliably operate regardless of changes in its characteristic length. For example, if the reactive component of the acoustic impedance of the load changes. However, it should be noted that a barbell-shaped horn, due to the large diameter of its output surface, produces a plane wave in water at cavitation, during the radiation of which the reactive component of radiation impedance is virtually absent.

#### 4. Experimental

For the experimental verification of the described horn design principles we have chosen the barbell-shaped horn shown in Fig. 7. Direct calorimetric measurement of acoustic energy transmitted by this horn into water at cavitation was selected as a method of this horn's performance evaluation. The measurements of the acoustic energy absorbed in the cavitation region were conducted with the apparatus shown in Fig. 8. Settled tap water at a temperature of

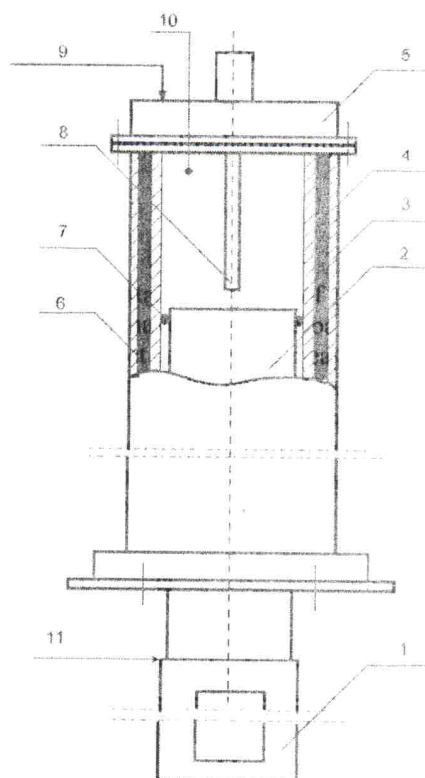


Fig. 8. Schematic of acoustic calorimeter is presented. 1 - magnetostrictive transducer, 2 - replaceable horn-radiator, 3 - external wall of calorimeter, 4 - heat insulation gasket, 5 - cover with porous sound-absorber, 6 - internal wall of calorimeter, 7 - scaling ring, 8 - set of thermocouples, 9 - gas supply, 10 - microphone, 11 - point of control over amplitude of transducer vibrations.

input resistance on frequency is a positive property because when several horns are connected in series, the analogous total dependence for the string will be also low. For horns with a gain factor greater than unity, the lowest dependence of the input resistance on frequency is displayed by

20 °C was used. The apparatus was based on an acoustic radiator consisting of a titanium horn connected to a magnetostrictive transducer, which operated at the resonance frequency of 17.8 kHz. The working power of the ultrasonic generator coupled to the magnetostrictive transducer was 5 kW. The oscillation amplitude of the magnetostrictive transducer was kept constant in all experiments at 1.67 m/s (rms). It was measured by placing a magnetic ring with an inductive coil on the transducer next to its output surface. Voltage was created in the coil as the transducer oscillated. The amplitude of this voltage corresponded to the oscillation amplitude and was measured by an oscilloscope. Prior calibration of this device was performed, in which the vibration amplitude was measured directly by a microscope.

A set of replaceable barbell-shaped horns was constructed to provide the necessary stepped change in the amplitude of the oscillatory velocity of the output end in contact with water. The set consisted of nine such horns with different gain factors (greater or smaller than unity), all of which had equal input and output diameters of 60 mm. Maximum oscillation velocity of some of these horns reached very large values, close to maximum theoretically possible for the best titanium alloys. Greatest achieved oscillation velocity was 12 m/s (rms). Therefore, maximum gain factor for the set was 7.2.

Static pressure in the calorimeter was produced with compressed nitrogen. The measurements of the resulting temperature of water were performed using a set of thermocouples. A change in the temperature of water during ultrasonic treatment was not more than 2–5 °C.

Fig. 9 shows an experimentally obtained plot of the specific acoustic power absorbed in the cavitation area, as a function of the oscillatory velocity of the horns' output radiating surfaces, at a static pressure of 1 bar. For the purpose of the measurement precision evaluation, data from Ref. [9] is also provided in the figure for the acoustic radiation frequency of 19 kHz and the static pressure of 1 bar.

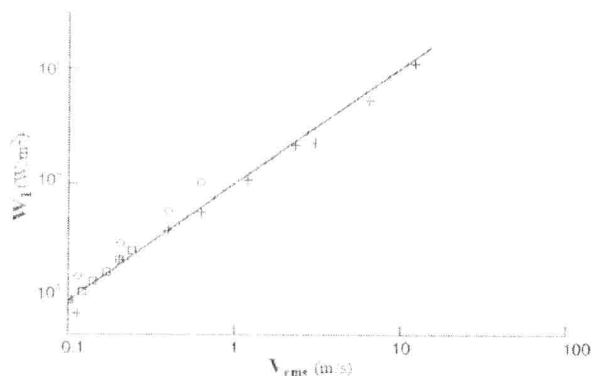


Fig. 9. Dependence of the intensity of the acoustic energy absorbed in the cavitation area is presented as a function of the oscillation velocity of the horns' output surfaces for a set of nine horns with different gain factors (+ are the data points from this work for the load pressure of 1 bar, o are the data points from this work for the load pressure of 2 bars, □ are the data points from Ref. [9]).

The figure shows that the experimental data obtained in this work in the small oscillation velocity range corresponds very well to the data from Ref. [9]. Unfortunately, for large vibration velocities, no literature data was found. Performance verification of the horns with different gain factors conducted during the experiments showed that all of them possessed resonance and gain characteristics well corresponding to the theoretically predicted values. In no case was it necessary to make any adjustments to the horns after they were originally machined.

Fig. 9 additionally shows a curve corresponding to the Eq. (3),  $W_1 = 0.5r_w V^2 = r_w V_{rms}^2 = P_0 V_{rms}$ . The fact that the experimental data follows the curve very well shows that the relationship,  $r_w V = \sqrt{2P_0}$ , suggested in Ref. [9] and verified there for the small oscillation velocities, is maintained also for the significantly larger oscillation velocities. Thus, it has been experimentally proven that the matching between our barbell-shaped acoustic horns and water at cavitation truly takes place, in accordance with the theory presented above, for all possible oscillation velocities of the horns' output surfaces.

To demonstrate the effect of the elevated static pressure, Fig. 9 also shows the experimental data corresponding to the static pressure of 2 bars. It is clearly seen that increasing the pressure augments the absorbed acoustic energy in the cavitation area.

The region of the specific power with the values above  $10^5 \text{ W/m}^2$  is very little studied, especially from the technological standpoint. The reason for this, from our perspective, is that the traditional cone-shaped horns, widely used in ultrasonic technology, are incapable of providing a large total radiation power, since their oscillation amplitudes are inversely proportional to the areas of their output surfaces. At large gain factors, the output surface area becomes very small, which complicates the development of sonochemical reactors capable of processing significant volumes of liquids. Thus, for example, a traditional stepped horn having an input diameter of 60 mm and a gain factor of 7.2 has the output diameter of, approximately, 20 mm. Therefore, at the maximum experimentally achieved specific power of  $10^6 \text{ W/m}^2$ , this stepped horn is capable of depositing not more than 300 W into its liquid load. Our barbell-shaped horn, used in the experiments presented in this section, on the other hand, delivers, approximately, 2.7 kW of total power, providing a power transfer efficiency increase by almost an order of magnitude.

A well-known method, described in detail in Ref. [12], was used for the experimental verification of the chemical activity in the cavitation area. The chemical activity level was determined by monitoring the oxidation reaction of KI in aqueous solution, resulting in the formation of free iodine. The obtained data is presented in Fig. 10. It can be clearly seen that the specific (divided by the horn's output surface area) rate of the concentration of the free iodine formation in the cavitation volume increases with the augmented intensity of the acoustic radiation. Total increase of the concentration of the reduced iodine at max-



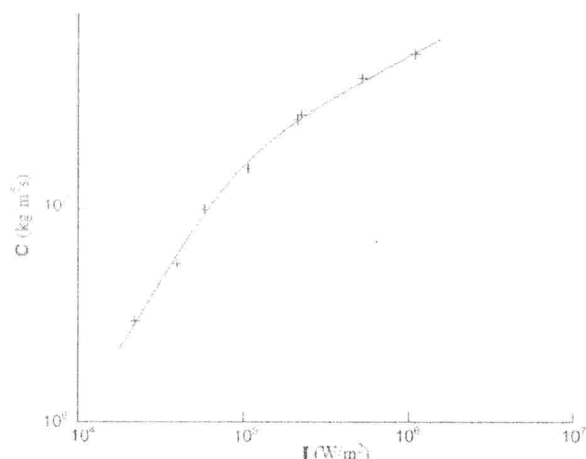


Fig. 10. Dependence of the specific (divided by the horn's output surface area) rate of the concentration of the free iodine formation in the cavitation volume is shown as a function of the intensity of the absorbed acoustic radiation.

534 imum intensity of acoustic radiation of  $10^6 \text{ W/m}^2$  reaches  
 535  $1.5 \times 10^5 \text{ kg/m}^3 \text{ s}$ .

536 **5. Conclusions**

537 Matching an ultrasonic transducer to a load is a matter  
 538 of choosing the matching horn that ensures the expression  
 539 (4) at a given gain factor  $G$ , and of subsequent calculation  
 540 of its resonance dimensions with the use of the system of  
 541 Eq. (9). As stated above, when matching to an active acous-  
 542 tic load with  $k_1 \ll 1$ , the standing acoustic wave in the trans-  
 543 ducer and in the horn is not disturbed, and their resonance  
 544 dimensions do not change. The most powerful horn, from  
 545 the designs described above, is the barbell-shaped horn,  
 546 which was chosen for the experimental investigations. Dur-  
 547 ing the experiments, performance evaluation of a set of such  
 548 horns with different gain factors showed that all of them  
 549 had the resonance and the gain factor characteristics that  
 550 corresponded very well to those predicted theoretically. It  
 551 was also experimentally verified that matching of the acous-  
 552 tic horns with water at cavitation, according to the theory  
 553 described above, is truly established for all possible values  
 554 of the output oscillation velocities of the horns.

555 It should be noted that matching an acoustic transducer  
 556 to a load using an acoustic horn is not the only possible  
 557 method of matching. Another powerful matching factor,  
 558 which results from the specific properties of water at cavi-  
 559 tation, is hydrostatic pressure  $P_0$ , according to the expres-  
 560 sion (6) and the experimental results presented here. It was  
 561 also previously theoretically demonstrated that an increase  
 562 in the load's hydrostatic pressure leads to an augmentation  
 563 of the intensity of acoustic radiation [13], further resulting  
 564 in an increase in the technological effectiveness of cavi-  
 565 tation. It is evident that the best results are obtained when  
 566 these two matching techniques are used jointly.

567 In conclusion, we would like to point out that our bar-  
 568 bell-shaped horns also perform well in low-viscosity non-  
 569 aqueous liquids and solutions, and permit building very  
 570 effective sonochemical reactors for conducting experiments  
 571 with these systems. This makes the described technology  
 572 very attractive for the studies involving the effect of the sec-  
 573 ond-order cavitation [14,15], which has been receiving a lot  
 574 of attention recently.

575 **References**

[1] A. Shoh, IEEE Trans. Sonics Ultrasonics su-22 (1975) 60. 576  
 [2] T.J. Mason, Ultrason. Sonochem. 10 (2003) 175. 577  
 [3] U.S. Bhirud, P.R. Gogate, A.M. Wilhelm, A.B. Pandit, Ultrason. 578  
 Sonochem. 11 (2004) 143. 579  
 [4] E. Eisner, in: W.P. Mason (Ed.), Methods and Devices, Part B, vol. 1, 580  
 Academic Press, New York, 1964. 581  
 [5] S. Sherrit, S.A. Askins, M. Gradziol, B.P. Dolgin, X.B.Z. Chang, Y. 582  
 Bar-Cohen, in: Proceedings of the SPIE Smart Structures Conference, 583  
 San Diego, CA 4701, Paper No. 34, 2002. 584  
 [6] J.W. Rayleigh (Strutt), The Theory of Sound, New York, 1945. 585  
 [7] A. Gallego-Juárez, G. Rodríguez-Corral, E. Riera-Franco de Sarabia, 586  
 C. Campos-Pozuelo, F. Vázquez-Martínez, V.M. Acosta-Aparicio, 587  
 Ultrasonics 38 (2000) 331. 588  
 [8] Y. Kikuchi, in: Y. Kikuchi (Ed.), Ultrasonic Transducers, Corona 589  
 Publ. Co., Tokyo, 1969. 590  
 [9] K. Fukushima, J. Saneyoshi, Y. Kikuchi, Ultrasonic Transducers, in: 591  
 Y. Kikuchi (Ed.), Corona Publ. Co., Tokyo, 1969. 592  
 [10] E.F. Neppiras, Ultrasonics 3 (1965) 9. 593  
 [11] L.G. Merkulov, A.B. Kharitinov, Sov. Phys. Acoust. (1959) 183. 594  
 [12] Sin Pin Lin, J. Acoust. Soc. Am. 36 (1964) 5. 595  
 [13] L.D. Rosenberg (Ed.), High-intensity Ultrasonic Fields, Plenum 596  
 Press, New York, 1971. 597  
 [14] R.P. Taleyarkhan, C.D. West, J.S. Cho, R.T. Lahey Jr., R.I. 598  
 Nigmatulin, R.C. Block, Science 295 (2002) 1868. 599  
 [15] D.J. Flannigan, K.S. Suslick, Nature 434 (2005) 52. 600  
 601